Ultrasound Images of Gray Contrast Tissue-mimicking Phantom

Haijiang Zhu[1], Wenjuan Li[1], Xin Wen[1], Ping Yang[2], Jinglin Zhou[1] and Jing Wang[1]

1. College of Information Science &Technology, Beijing University of Chemical Technology, Beijing, 100029, China
E-mail: zhuhj@mail.buct.edu.cn

2. Division of Mechanics and Acoustic, National Institute of Metrology, Beijing, 100029, China
E-mail: yangp@nim.ac.cn

Abstract: This paper prepared a tissue-mimicking ultrasound phantom to test the contrast of ultrasonic equipment and presented the analysis of ultrasound image based on support vector machine (SVM). The gray contrasts in the tissue-mimicking phantom are regulated by changing scatter particles aluminum and corn starch. Embedded at depths of 3, 5, 7, 9, 11, and 13cm were set of cylindrical inclusions, not including scatter particles, in the axial direction. Six cylinder inclusions, containing tissue-mimicking material with a different scatter size and number density, were set in the lateral direction. Attenuations and backscatter coefficients of the background and the cylinder targets are independently measured to verify the phantom. Images obtained while scanning the prepared phantom with ultrasound diagnostic systems are available to test the gray contrast of the phantom. Furthermore, the gray contrast between cylindrical inclusions and background material is estimated for ultrasound image. And the cylinder targets segmentation based on the SVM method is performed for ultrasonic image. The experimental result shows that the prepared phantom can be utilized to test ultrasound diagnostic systems.

Key Words: Gray contrast; image segmentation; SVM; ultrasound phantom.

1 INTRODUCTION

Ultrasound is often considered the preferred imaging modality because of its ability to provide continuous, real-time images without the risk of ionizing radiation and at a lower cost than computed tomography (CT) or magnetic resonance imaging (MRI) [1]. Therefore, the development of ultrasonic instrument is very fast. It establish as a medical imaging device in the 1960s. Multichannel systems with electronic control of transducer arrays were developed in 1970s. In the 1980s, Doppler ultrasound was invented [2]. To today, the application of ultrasonic instrument is becoming more and more extensive. In the medical field, ultrasonic instrument has become one of the indispensable instruments in the hospital, which provides a good basis for the diagnosis [3]. Ultrasound equipment in different medical applications has emerged as the times require. Traditional ultrasonic equipment is very effective for the detection of fetal detection and liver and other organs, Doppler ultrasound is used to measure blood and tissue velocities in cardiac, vascular and other tissues [4], elastography visualizes the deformation behavior of a tissue in response to an externally applied mechanical compression [5], Synthetic aperture ultrasound imaging has recently developed as a promising tool to improve the capabilities of medical ultrasound [6], Nanodroplet-mediated histotripsy [7] is also the application of clinical ultrasound. Therefore, the quality of the ultrasonic device directly affects the doctor's diagnosis results of the safety of the patient.

This work was part supported by the National Natural Science Foundation of China under grant No. 61473025 and No. 61573050, the Fundamental Research Funds for the Central Universities (YS1404).

The development of ultrasonic tissue-mimicking phantom has many different kinds of phantom, which focus on different aspects, and there are many people who study the acoustic parameters of ultrasonic phantom in order to better detect ultrasonic equipment or to get more information from ultrasonic images. For example, the quantitative ultrasound method can better describe many diffusion diseases, such as fatty liver, blood vessel hypertrophy, but also clear areas of rat mammary fibroadenomas and 4T1 mouse carcinomas [8]. Quantitative ultrasound technique utilizes the amplitude and frequency dependence of the backscatter coefficient (BSC) to estimate the size and concentration of scatters [9, 10, 11]. An essential task in all medical imaging is the detection of focal lesions against background tissue within individual organs [12, 13]. So backscatter, attenuation, focal lesions against background and effective frequency are the factors that influence the ultrasonic image, and it is also a very much studied acoustic parameters. Wilson [14] discusses the relationship between backscattering and contrast.

In this paper, a tissue-mimicking ultrasound phantom is designed to test the contrast of ultrasonic equipment. Unlike gray scale ultrasound phantom [15], gray contrasts of ultrasound image are regulated by changing scatter particles aluminum and corn starch in the improved ultrasound phantom. In addition, the analysis of the ultrasonic image of the prepared phantom is carried out through estimating the gray contrast between cylindrical inclusions and background material and the cylinder targets segmentation based on the SVM method. The experimental result validates that the designed phantom is available to test medical ultrasonic instrument.

The rest of this paper is structured as follows. The ultrasound phantom is designed and prepared, and the cylinder inclusions segmentation based on SVM is presented in Section 2. Section 3 is the experimental results on attenuation and backscatter coefficients measurement, and analysis of ultrasound image of the phantom. Finally, the conclusion is outlined in Section 4.

2 MATERIALS AND METHODS

2.1 Ultrasound Phantom Design

It is similar to literature [15], and the size of the ultrasound phantom is $20\times6\times15$ cm (see in Fig 1). One column and one row of the round thru-hole (cylinder) with diameter 1 cm are displayed in the ultrasound phantom. The column role is to test the probing depth of ultrasound instrument, and they usually are anechoic under ultrasound. The row role including seven is to test the gray contrast of ultrasound instrument, and they are applied to evaluate target contrast levels by computing ratio of the integrated backscatter signal intensity (IBSI) for the background material and the targets[14].

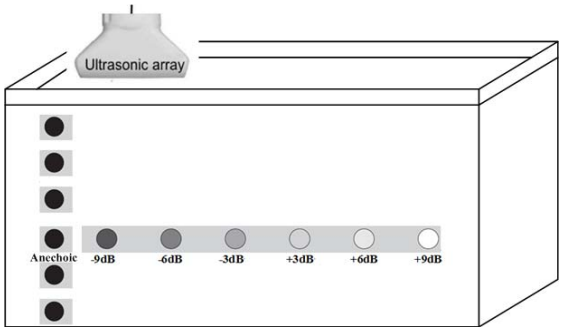

Fig 1. The diagram of the phantom

2.2 Preparation of Ultrasound Phantom

The tissue-mimicking ultrasound phantom is made of the background material and the target an aqueous gel. Embedded at depths of 3, 5, 7, 9, 11, and 13cm were set of cylindrical inclusions in the axial direction, and each inclusion does not include scatter particles. At the depth 9 cm, six cylinder inclusions in a row were set in the lateral direction and each containing tissue-mimicking material with a different scatter size and number density. This aqueous gel [16] includes polyacrylamide (Tianjin, China), ammonium persulfate (Tianjin, China) and so on. Corn starch (Beijing, China) and aluminum (Shanghai, China) is regarded as scatter particles in the improved ultrasound phantom.

The gray contrast tissue-mimicking ultrasound phantom is composed of the background material and the cylinder target material at different positions. The cylinder target contrast levels can be evaluated by estimating ratio of IBSI (f_{center}) for the background material and the targets using a decibel scale [14]. That is to say, the computing model is written as

Target contrast (dB) =

$$10\log\left[\frac{IBSI(f_{center})target}{IBSI(f_{center})background}\right] \quad (1)$$

The attenuation of the background material is controlled the mixture of aluminum particles with diameter 0.5 μm and 3 μm. The attenuation of the cylinder targets with seven levels are controlled the mixture of aluminum and cone starch. The diameter of aluminum particles are 0.5 μm, 3 μm, 7 μm, 10 μm and 100~200 meshes.

Table1. Scatter particle components used to prepare the background and the target.

	Background material	Anechoic	-9dB	-6dB	-3dB	+3dB	+6dB	+9dB
Cone starch	—	—	0.02%	0.2%	—	—	—	—
Aluminum 0.5 μm	1%	—	—	—	—	0.3%	1.5%	—
Aluminum 3 μm	1%	—	—	—	—	0.3%	3.5%	—
Aluminum 7 μm	—	—	—	—	0.5%	—	—	—
Aluminum 10 μm	—	—	—	—	0.5%	—	—	3%
Aluminum 100~200 meshes	—	—	—	—	—	—	—	4%

("—" represents for "Null".)

The attenuations and backscatter coefficients of the background material and the cylinder targets in produced phantom are measured through the pulse insertion substitution method and the pulse echo method.

The pulse insertion substitution method is applied to measure attenuation of the background material and the cylinder targets. Attenuation can be measured by

$$\alpha=\frac{20\log(A_1/A_2)}{d_1-d_2}+\alpha_1 \quad (2)$$

where the α and α_1 are the attenuation of TM material and water, respectively, A_1 and A_2 are the amplitude of the received signal when change the thickness of TM material, d_1 and d_2 the thickness the transducer pass the TM material. For the attenuation of water is too small to affect the result, so equation (2) can be written as

$$\alpha=\frac{20\log(A_1/A_2)}{d_1-d_2} \quad (3)$$

The pulse echo method is utilized to measure backscattering coefficient. In order to avoid the error

caused by the different position of the organization, the ultrasonic tissue material has a flat surface to be as small as possible and as smooth as possible. BSC can be calculated by

$$\eta(\omega)=\frac{\left\langle\left|v_s(r\in v;\omega)\right|^2\right\rangle}{\left|v_{ref}\left(2z_{ref};\omega\right)\right|^2} \tag{4}$$

Where $\left\langle\left|v_s(r\in v;\omega)\right|^2\right\rangle$ means the average power spectra of the echo signal from TM material; $\left|v_{ref}\left(2z_{ref};\omega\right)\right|^2$ means the power spectra of echo signal from the rigid plane reflector; z_{ref} is the distance between the transducer and the rigid plane reflector; r is the distance between the scatter and transducer; v is an area of TM phantom; ω is the natural angular frequency of the transducer.

2.3 Image segmentation based on SVM

The motive of the prepared gray contrast phantom is to recognize the cylinder inclusions of ultrasonic image. Therefore, we should detect the cylinder targets from different gray intensities when the phantom is scanned by medical ultrasonic instrument. Support vector machine (SVM) has been applied widely in data analysis, pattern recognition, and classification. In recent years, SVM is also used in the ultrasound image segmentation [16-19]. The cylinder targets segmentation based on the SVM method is presented for ultrasound image of the produced phantom in this section. Here, this section utilizes the LIBSVM tool [20] to perform the segmentation of the cylinder inclusions of ultrasonic image. This method is outlined as follows:

1) Selected a region of interest including one cylinder target in the ultrasound image.
2) Sampled two groups of training data in the foreground image and the background image. The training data are constituted by the pixel intensity of the foreground and background image.
3) Established the support vector model from the training data using the function svmtrain () in the LIBSVM tool [20].
4) Segmented the cylinder inclusion in the light of the models set up in step 3) using the function svmclassify () in he LIBSVM tool [20].
5) Labeled the cylinder inclusions in the light of the segmented results.
6) Threshold image is obtained from the labeled result.
7) Deleted a few tiny areas except the object using mathematical morphology.
8) Extracted the contour of the cylinder inclusions.

In this method, the type of SVM is set as C-SVC and the type of kernel function is selected as the radial basis function.

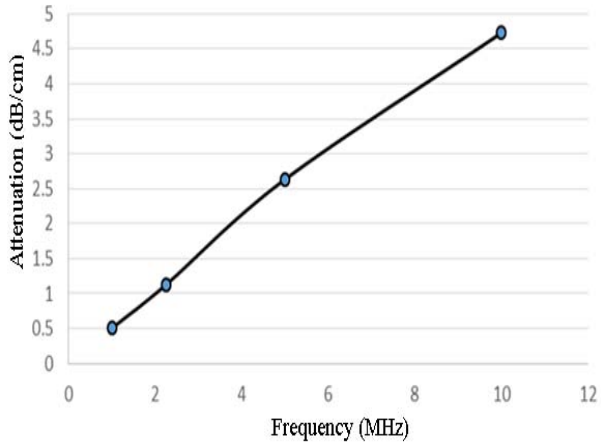

Fig 2. The measured attenuation of the background material.

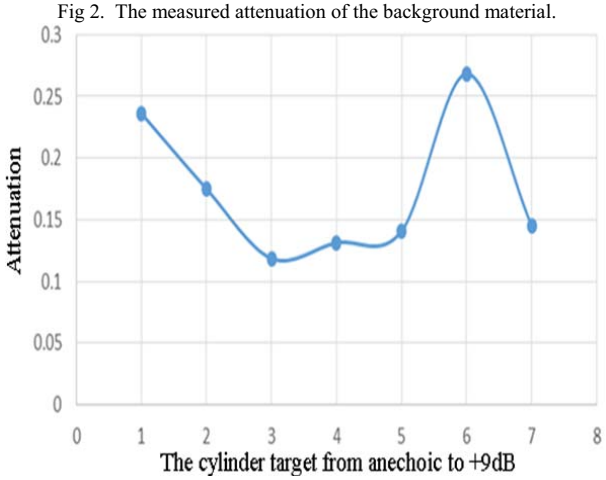

(a)

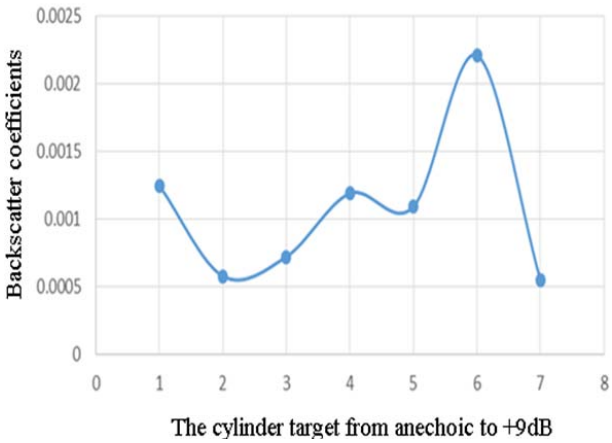

(b)

Fig 3. The measured attenuations (a) and backscatter coefficients (b) of the cylinder targets.

3 RESULTS

3.1 Attenuation and Backscatter Coefficient Measurements.

In the experiment, attenuation of the background material was firstly measured at different frequencies. The experiments were carried out using nominal frequency settings of 1MHz, 2.25MHz, 5MHz and 10MHz. Fig 2 presents the measured attenuation of the background

material. Attenuations of the background material are linear with frequency, and their values are almost 0.5 $dB \cdot cm^{-1} \cdot MHz^{-1}$ in this chart. Then, attenuation and backscatter coefficient of the cylinder targets are estimated when frequency of the transducer is 5.0 MHz. We can observe that the backscattering coefficient and attenuation of the cylinder targets with seven levels have the same variation trend.

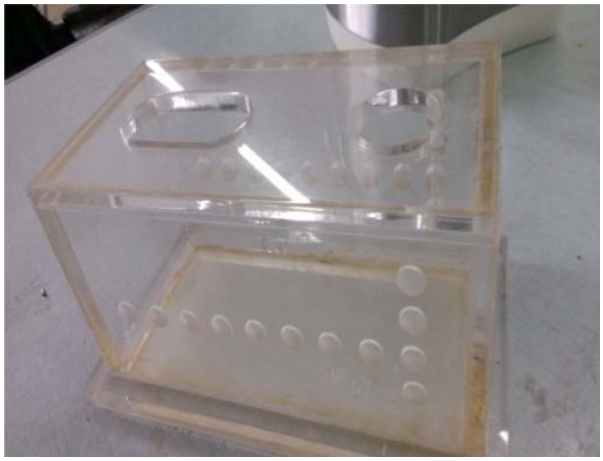

(a)

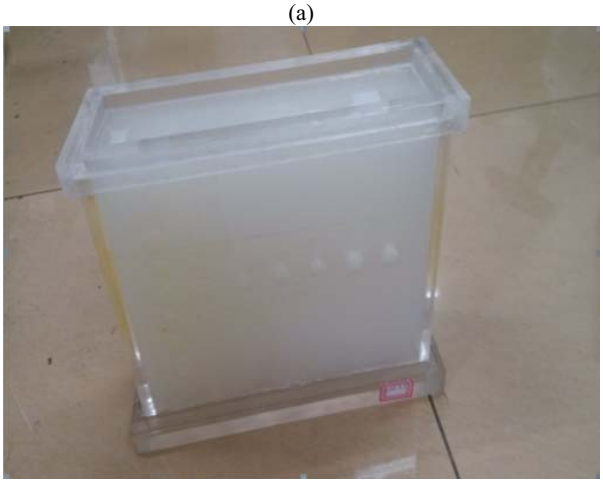

(b)

Fig 4. The mould (a) and the prepared ultrasound TM phantom with gray contrast (b).

3.2 Phantom ultrasound Images

Fig 4 shows the mould and the prepared ultrasound phantom with seven gray contrasts. The ultrasound RF signals of the phantom were recorded using a SonoScape ultrasound system (SonoScape, Co., Ltd, Shenzhen, China), equipped with a linear array transducer. Images were obtained using nominal frequency settings of 5.0 MHz, and two of these ultrasound images were shown in Fig 5. Fig 5 (a) displays the image of the phantom for the shallow focus, where a few cylinder targets were not observed. The ultrasound image of the lateral cylinder targets named as +9dB through -9dB from right to left are illustrated by the red arrows in Fig 5 (b) while the focus of the ultrasound system is deeper. These contrast levels correspond to an effective imaging frequency of 5.0MHz for the shallow focus and the deeper focus. This experiment illustrates how the ultrasound phantom can be utilized for quantitative measurements of the equipment.

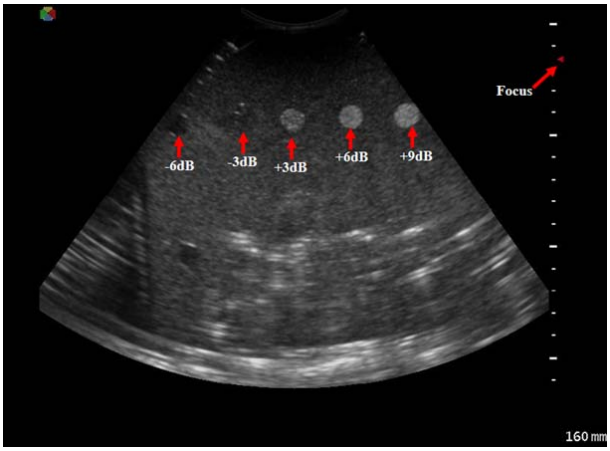

(a)

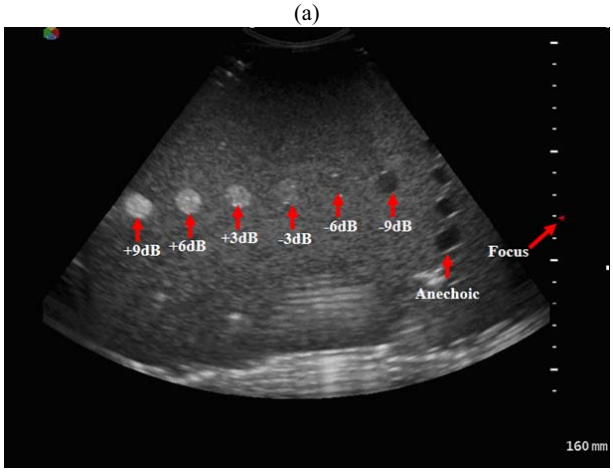

(b)

Fig 5. Set of images obtained by a SonoScape scanner of the phantom at 5.0 MHz frequency for the shallow focus (a) and the deeper focus (b). Cylinder targets are shown by the red arrows.

Fig 6 shows the diagram of the seven gray contrasts for images of the cylinder targets and the background material. Firstly, the regions of interest in the image of the cylinder targets are marked as red rectangle in Fig 6. Secondly, the same rectangles are selected (marked by white rectangle) in the image of the background materials. In this experiment, we random choose ten rectangle regions in the background image. After estimating the intensity sum of these rectangles, the gray contrasts are computed for seven cylinder targets. The mean of the intensity ratios are listed in Table 2. It is obvious that the changes in gray contrasts observed in Fig 6 are more consistent with the estimated intensity ratios. When the phantom is scanned by the ultrasound system at the shadow focus in Fig 5 (a), the intensity ratios have a few variations. However, the gray contrast levels are almost the same as the image obtained by the deeper focus.

Fig 7 presents the diagram of the segmentation of the cylinder target using the SVM method. First, the cylinder inclusion and the background are sampling in order to obtain the trained model. The data marked by yellow “o” and red “*” in Fig 7 are training samples. Then, the function svmtrain () and svmclassify () in he LIBSVM tool [20] are

applied to segment the object and the background and the result is displayed in second and third column of Fig 7. The tiny areas in the third column are deleted using mathematical morphology. Finally, the border of the cylinder target is extracted from the segmented result. From these results, we can see that the object is distinguished from the background image when their intensity has a larger difference.

Table2. The mean of the intensity ratios for the cylinder targets and the background material.

	Anechoic	-9dB	-6dB	-3dB	+3dB	+6dB	+9dB
Intensity ratio in Fig.5(a)	Null	Null	0.788	0.902	1.214	1.627	1.726
Intensity ratio in Fig.6	0.529	0.667	0.946	1.112	1.480	1.667	1.705

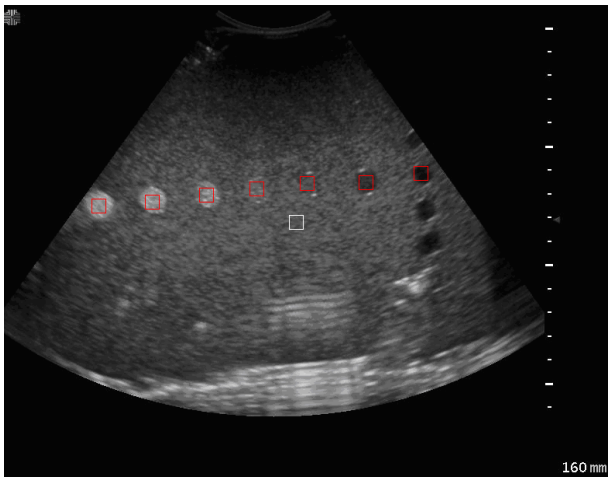

Fig 6. The diagram of the estimated gray contrast between image of the cylinder targets and image of the background material.

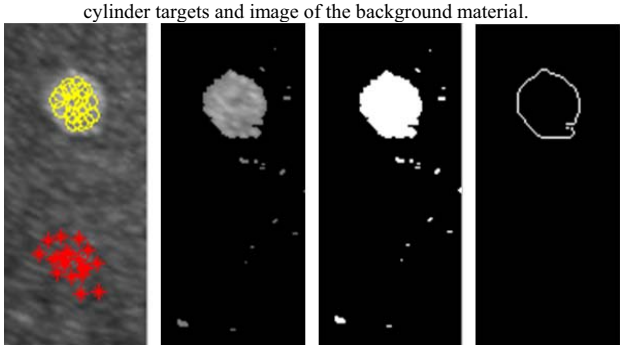

Fig.7. Segmentation of the cylinder target based on SVM. From left to right: Sampling in background (red "*") and foreground (yellow "o"), the segmented result, the binaryzation result, the contour curve.

Fig.8 is the segmented result of ultrasonic image of the phantom using the SVM method. Two of all cylinder inclusions are not extracted using the SVM method. This is because intensities of the two targets and background do not have much difference. And the classified model is unlikely to obtain from training data in the SVM method. These results show that the cylinder targets with high contrast are extinguished from ultrasonic image.

Fig.9 is the fitted circles of the cylinder inclusions in ultrasonic image from the segmented result shown as Fig.8. These green circles are drawn using the least squares method. From these fitted results, we can see that most of the cylinder targets is segmented using the SVM method. These results indicate the segmentation of the cylinder inclusions based on SVM method in ultrasonic image.

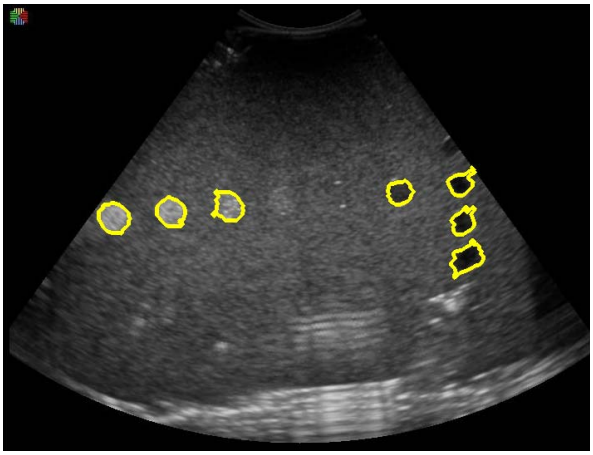

Fig.8. The segmented result of the cylinder targets in ultrasonic image of the phantom.

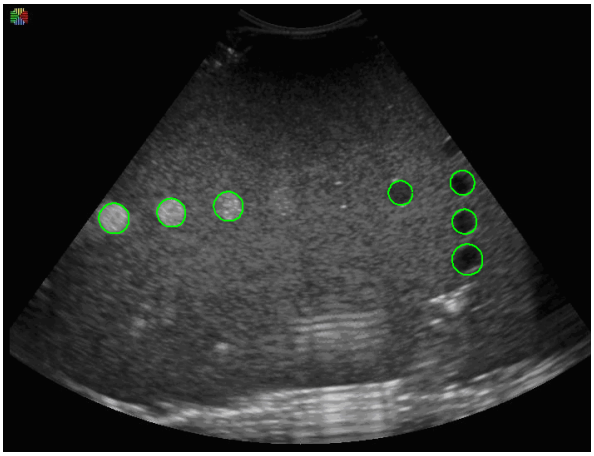

Fig.9. The fitted circles of the cylinder targets in ultrasonic image from the segmented result displayed in Fig.8.

4 CONCLUSIONS

This work has designed and prepared an improved gray contrast ultrasound phantom for detecting medical ultrasonic instrument and has discussed the analysis of ultrasound image based on support vector machine (SVM). The gray contrasts of ultrasound image were controlled by changing scatter particles aluminum and corn starch. We measured attenuation and backscatter coefficient of the preparation phantom. The gray contrasts for images of the cylinder targets and the background material in ultrasound phantom were computed and discussed in the experiments. In addition, the cylinder targets segmentation based on the SVM method was performed for ultrasonic image. The

tested results by clinical systems on the ultrasound images of the phantom indicated feasibility.

REFERENCES

[1] A. Mayani, Development of a Routine Objective Quality Control Program for Diagnostic Ultrasound, University of Florida, 2002.

[2] J. Bercoff, Ultrafast ultrasound imaging, INTECH Open Access Publisher, 4-24, 2011.

[3] S. Lee, J. I. Choi, M. Y. Park, D. M. Yeo, J. Y. Byun, S. E. Jung et al, Intra-and interobserver reliability of gray scale/dynamic range evaluation of ultrasonography using a standardized phantom. Ultrasonography, Vol.33, No.2, 91-97, 2014.

[4] A. Walker, Performance testing of ultrasound Doppler equipment. Linköping Studies in Science and Technology, 2003.

[5] E. Brusseau, C. Perrey, P. Delachartre, M. Vogt, D. Vray and H. Ermert, Axial strain imaging using a local estimation of the scaling factor from RF ultrasound signals. Ultrasonic imaging, Vol.22, No.2, 95-107, 2000.

[6] L. Huang, Y. Labyed, F. Simonetti, M. Williamson, R. Rosenberg, P. Heintz, D. Sandoval, High-resolution imaging with a real-time synthetic aperture ultrasound system: A phantom study, SPIE Medical Imaging, International Society for Optics and Photonics, 79681I-79681I, 2011.

[7] E. Vlaisavljevich, O. Aydin, Y. Y. Durmaz, K. W. Lin, B. Fowlkes, M. ElSayed, Z. Xu, Effects of Ultrasound Frequency on Nanodroplet-Mediated Histotripsy, Ultrasound in Medicine and Biology, Vol.41, Iss.8, 2135-2147, 2015.

[8] K. Nam, I. M. Rosado-Mendez, L. A. Wirtzfeld, G. Ghoshal, A. D. Pawlicki, E. L. Madsen, et al, Comparison of ultrasound attenuation and backscatter estimates in layered tissue-mimicking phantoms among three clinical scanners. Ultrasonic Imaging. Vol. 34, No. 4, 209-211, 2012.

[9] E. J. Boote, J. A. Zagzebski, E. L. Madsen, Backscatter coefficient imaging using a clinical scanner, Medical Physic. Vol.19, No.5, 1145-1152, 1992.

[10] E. Walach, A. Shmulewitz, Y. Itzhak, Z. Heyman, Local tissue attenuation images based on pulsed-echo ultrasound scans, IEEE transactions on biomedical engineering, Vol.36, No.2, 211-221, 1989.

[11] E. Franceschini, R. Guillermin, F. Tourniaire, E. Lamy, S. Roffino, J. F. Landrier, On the use of the Structure Factor Model to understand the measured backscattercoefficient from concentrated cell pellet biophantoms, IEEE International Ultrasonics Symposium, 1220-1223, 2013.

[12] S. W. Smith, R. F. Waner, J. M. Sandrik, H. Lopez, Low contrast detectability and contrast/detail analysis in medical ultrasound. IEEE transactions on sonics and ultrasonics, Vol.30, No.3, 164-172, 1983.

[13] J. J. Rownd, E. L. Madsen, J. A. Zagzebski, G. R. Frank, F. Dong, Phantoms and automated system for testing the resolution of ultrasound scanners, Ultrasound in medicine & biology, Vol.23, No.2, 245-259, 1997.

[14] T. Wilson, J. Zagzebski, Y. Li, A test phantom for Estimating changes in the effective frequency of an ultrasonic Scanner, Journal of ultrasound in medicine, Vol.21, No.9, 937-945, 2002.

[15] http://www.cirsinc.com/products/modality/73/gray-scale-ultrasound-phantom/

[16] T. Lin, Q. Jin, H. Yao and H. Zheng, Preparation and characterization of a new ultrasound tissue-mimicking phantom, Bulletin of advanced technology research, 29-33, 2010.

[17] Y. Artan, M.A.Haider, D.L.Langer, T.H.Van Der Kwast, A.J.Evans, Y.Yang, M.N.Wermick, J.Trachtenberg and I.S.Yetik, Prostate cancer localization with multispectral MRI using cost-sensitive support vector machines and conditional random fields, IEEE Transactions on Image Processing, Vol.19, No.9, 2444-2455, 2010.

[18] H. Yang, X. Zhang, X. Wang, LS-SVM-based image segmentation using pixel color-texture descriptors, Pattern Analysis and Applications, Vol.17, Iss.2, 341-359,2014.

[19] C. Wu, C. Lai, C. Chen, Y. Chen, Automated Clustering by Support Vector Machines with a Local-Search Strategy and its Application to Image Segmentation, Optik-International Journal for Light and Electron Optics,Vol.126, Iss.24, 4964–4970, 2015.

[20] C. C. Chang, C. J. Lin, LIBSVM: A library for support vector machines. ACM Transactions on Intelligent Systems and Technology Vol.2, Iss.3, 2011.